

1 **Improved Robustness of SARS-CoV-2 Whole-Genome Sequencing from**
2 **Wastewater with a Nonselective Virus Concentration Method**

3
4 Emily Segelhurst,¹ Jonathan E. Bard,^{2,3,6} Annemarie N. Pillsbury,¹ Md Mahbubul Alam,¹ Natalie
5 A. Lamb,² Chonglin Zhu,¹ Alyssa Pohlman,² Amanda Boccolucci,² Jamaal Emerson,⁴ Brandon J.
6 Marzullo,^{2,3} Donald A. Yergeau,² Norma J. Nowak,^{2,3} Ian M. Bradley,^{1,5} Jennifer A. Surtees,^{3,4,6}
7 Yinyin Ye^{1,*}

8
9 ¹Department of Civil, Structural and Environmental Engineering, University at Buffalo, Buffalo,
10 New York 14260, United States

11 ²UB Genomics and Bioinformatics Core, University at Buffalo, Buffalo, New York 14203,
12 United States

13 ³Department of Biochemistry, Jacobs School of Medicine and Biomedical Sciences, University
14 at Buffalo, Buffalo, New York 14203, United States

15 ⁴Department of Microbiology and Immunology, Jacobs School of Medicine and Biomedical
16 Sciences, University at Buffalo, Buffalo, New York 14203, United States

17 ⁵Research and Education in Energy, Environmental and Water (RENEW) Institute, University at
18 Buffalo, Buffalo, New York 14260, United States

19 ⁶Genetics, Genomics and Bioinformatics Graduate Program, Jacobs School of Medicine and
20 Biomedical Sciences, University at Buffalo, Buffalo, New York 14203, United States

21 _____
22 *Corresponding author: yinyinye@buffalo.edu

23 Tel. (716) 645-4002

26 **ABSTRACT**

27 The sequencing of human virus genomes from wastewater samples is an efficient method for
28 tracking viral transmission and evolution at the community level. However, this requires the
29 recovery of viral nucleic acids of high quality. We developed a reusable tangential-flow filtration
30 system to concentrate and purify viruses from wastewater for whole-genome sequencing. A pilot
31 study was conducted with 94 wastewater samples from four local sewersheds, from which viral
32 nucleic acids were extracted, and the whole genome of severe acute respiratory syndrome
33 coronavirus 2 (SARS-CoV-2) was sequenced using the ARTIC V4.0 primers. Our method yielded
34 a high probability (0.9) of recovering complete or near-complete SARS-CoV-2 genomes (>90%
35 coverage at 10× depth) from wastewater when the COVID-19 incidence rate exceeded 33 cases
36 per 100 000 people. The relative abundances of sequenced SARS-CoV-2 variants followed the
37 trends observed from patient-derived samples. We also identified SARS-CoV-2 lineages in
38 wastewater that were underrepresented or not present in the clinical whole-genome sequencing
39 data. The developed tangential-flow filtration system can be easily adopted for the sequencing of
40 other viruses in wastewater, particularly those at low concentrations.

41

42 **KEYWORDS**

43 SARS-CoV-2, COVID-19, whole-genome sequencing, tangential-flow filtration, wastewater-
44 based epidemiology

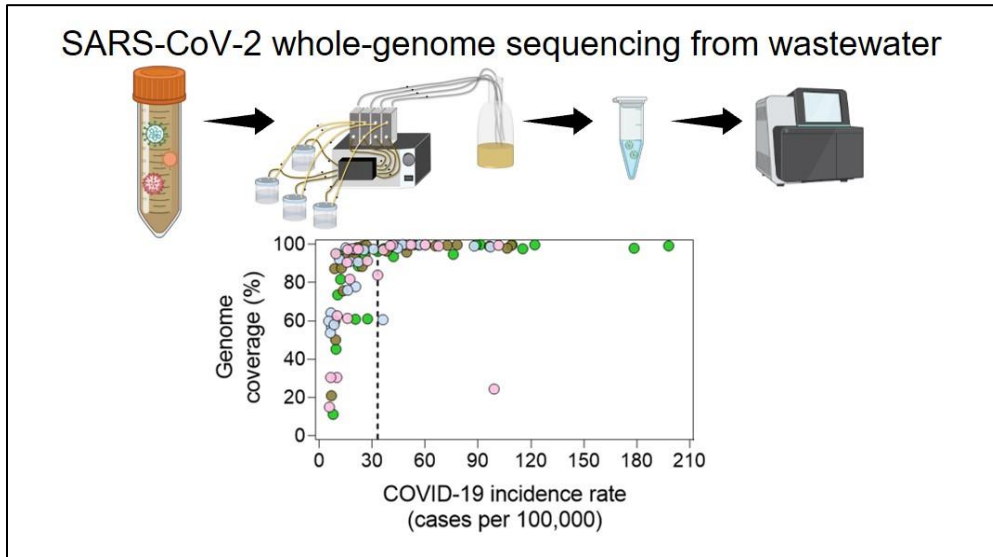
45

46 **SYNOPSIS**

47 The tangential-flow filtration method extracts viral nucleic acids of high enough quality from
48 wastewater for robust and successful whole-genome sequencing.

49

50 **GRAPHIC FOR TABLE OF CONTENTS (TOC)**



51

52

53 **INTRODUCTION**

54 The global spread of severe acute respiratory syndrome coronavirus 2 (SARS-CoV-2) has
55 facilitated the emergence of genome mutations, resulting in new lineages that further threaten
56 public health.¹ Whole-genome sequencing (WGS) of clinical samples is a powerful method for
57 tracking the spread of various SARS-CoV-2 lineages,² but this can be expensive, slow, and subject
58 to biased sampling. Furthermore, the frequency of clinical testing has declined, aided by the
59 availability of rapid at-home testing kits. WGS of SARS-CoV-2 in wastewater samples
60 circumvents the issues as a high-throughput and more comprehensive strategy that monitors a
61 larger portion of the population.³⁻⁶ Successful WGS of SARS-CoV-2 in wastewater samples relies
62 on the depth (the number of times a nucleotide is sequenced)⁷ and breadth of genome coverage
63 (hereafter, coverage; the percentage of nucleotide positions sequenced to a given depth).⁷ Because
64 SARS-CoV-2 lineages differ by only a few mutations, greater depth and coverage are needed to
65 quantify lineage abundance and detect low-frequency mutations.^{8,9}

66 Different virus concentration methods have been developed for polymerase chain reaction
67 (PCR)-based detection of viral genes from wastewater.¹⁰⁻¹³ However, the nucleic acids recovered
68 with these methods may not be suitable for WGS—PCR assays typically target <1% of the
69 genome. Sequencing inhibitors, such as humic acids, and background nucleic acids from
70 prokaryotes and eukaryotes are likely to reduce the genome coverage of SARS-CoV-2. Indeed,
71 near-complete (>90%) SARS-CoV-2 genomes are not recovered from most samples (>85%) when
72 aluminum hydroxide is used to directly precipitate viruses without separating viruses from other
73 microorganisms in wastewater.¹⁴ The removal of wastewater solids before the Amicon/Centricon
74 ultra-centrifugal concentration¹⁵ or electronegative membrane filtration¹⁶ can improve sequencing

75 success, but the quality of the extracted genomes can vary and random sequencing failures can
76 occur.¹⁷

77 We report a reusable and nonselective tangential-flow filtration system to concentrate and
78 purify viruses from wastewater for WGS. We evaluated the robustness of the method to recover
79 complete or near-complete SARS-CoV-2 genomes using the samples collected from four local
80 sewersheds over six months. We subsequently compared the findings with those from patient-
81 derived clinical samples at the County level. Finally, the timing of lineage detection was compared
82 among clinical WGS, wastewater WGS, and quantitative reverse transcription polymerase chain
83 reactions (RT-qPCR).

84

85 **MATERIALS AND METHODS**

86 **Wastewater sample collection**

87 Time- or flow-weighted 24-hr composite influent samples were collected every 1 or 2
88 weeks between October 1 and December 16, 2021, and between January 18 and April 12, 2022,
89 from three wastewater treatment plants covering four sewersheds that serve ~80% of the total
90 population of Erie County (New York): Tonawanda, Kenmore-Tonawanda, Amherst, and Bird
91 Island (**Table S1; Figure S1**). Influent was collected by an autosampler every 30 min, and the
92 samples were kept at 4 °C in high-density polyethylene bottles that were cleaned with 10% bleach.
93 The samples were transported on ice packs and stored at 4 °C until they were processed.

94

95 **Virus concentration from wastewater**

96 Wastewater samples (125 mL) were centrifuged in sterile bottles at $10\,000 \times g$ for 15 min
97 at 4 °C to remove large wastewater solids, prokaryotic and eukaryotic cells, and other debris. The

98 supernatant was concentrated in a Vivaflow laboratory cross flow cassette system (Sartorius)
99 equipped with a 30-kDa Hydrosart ultrafilter membrane (Sartorius) at a feedline flow rate of 8.5
100 mL/min (**Figure S2**). The residual liquid in the ultrafilter membrane and connected tubing was
101 blown with air into the sample reservoir. The concentrate (~25 mL) in the reservoir was then
102 collected, overlaid with 5 mL of a 20% (v/v) sucrose solution and ultracentrifuged at $100\,000 \times$
103 g for 45 min at 4 °C in an SW 32 Ti rotor using an Optima XE series centrifuge (Beckman Coulter).
104 Immediately after the ultracentrifugation, the pellet was resuspended in 200 μ L phosphate-
105 buffered saline (pH 7.4; Gibco) and stored at -80 °C ~two weeks until nucleic acid extraction.

106 After use, the ultrafilter membranes were immediately flushed with ~100 mL of 0.5 M
107 NaOH solution preheated to 55 °C at a feedline flow rate of 8.5 mL/min. The NaOH solution was
108 then recirculated for 20–30 min at the same flow rate. The cleaned membrane was stored in 0.5 M
109 NaOH at 4 °C. Cleaning efficiency was verified on six random days by processing 125 mL of
110 autoclaved Milli-Q water with the same concentration procedure. The absence of SARS-CoV-2
111 genes through washed filters were confirmed by RT-qPCR (**Figure S3**).

112

113 **Nucleic acid extraction and RT-qPCR**

114 Viral nucleic acids were extracted from the concentrated samples with QIAamp viral RNA
115 mini kits (Qiagen) and eluted in 60 μ L AVE buffer (Qiagen) per the manufacturer's instructions.
116 One-step RT-qPCR was performed to quantify the SARS-CoV-2 N gene according to the CDC
117 N2 assay¹⁸ and to determine the presence/absence of specific S gene mutations, including WT493-
118 498, Q493R and Q498R, delH69/V70, and delL24/P25/P26 and A27S as variant determinants for
119 Delta, generic Omicron, Omicron BA.1, and Omicron BA.2, respectively, following methods
120 published previously (**Table S2**).^{19, 20} The limit of detection for the SARS-CoV-2 N gene was

121 determined to be 1.8 gene copies/ μ L, and the limit of quantification was determined to be 5 gene
122 copies/ μ L following a method as described previously (**Figure S4**).²¹ A checklist of the MIQE
123 (minimum information for publication of quantitative real-time PCR experiments) guidelines²² is
124 provided in **Table S3**. All RT-qPCR assays were conducted in duplicates on a CFX96 Touch real-
125 time PCR detection system (Bio-Rad), and the threshold cycle (C_T) value was determined using a
126 CFX Maestro Software (Version 4.0, Bio-Rad). To remove PCR inhibition, the extracted nucleic
127 acids were diluted 5- or 10-fold in nuclease-free water before RT-qPCR analyses (**Figure S5**).
128 Detailed procedures of RT-qPCR inhibition test, reaction compositions, thermocycling conditions,
129 and determination of the limits of detection and quantification are described in the Supporting
130 Information.

131

132 **SARS-CoV-2 whole-genome sequencing (WGS)**

133 The quality of the extracted nucleic acids was assessed with the Agilent Fragment
134 Analyzer. WGS of SARS-CoV-2 was performed following a modified ARTIC protocol²³ using
135 the V4.0 nCOV-2019 amplicon panel (IDT). Briefly, 8 μ L of nucleic acid extracts was reverse
136 transcribed to cDNA with random hexamers using the Invitrogen SuperScript IV first-strand
137 synthesis system (Thermo Fisher Scientific) according to the manufacturer's protocol. The cDNA
138 was amplified with two primer pools using Q5 hot-start high-fidelity 2 \times master mix (New England
139 BioLabs) with the following parameters: 98 $^{\circ}$ C for 30 s, 25 cycles of 98 $^{\circ}$ C for 15 s and 65 $^{\circ}$ C for
140 5 min. The resulting amplicons from both primer pools were combined. Excess primers and
141 reagents were removed with 1 \times AMPure XP beads (Beckman Coulter), and the amplicons were
142 eluted in EB buffer (Qiagen). The total eluted volume of amplicons was input to generate libraries
143 using the NEBNext Ultra II DNA library prep kit (New England BioLabs) without fragmentation

144 per the manufacturer's protocol. Individual samples were then barcoded and pooled for
145 quantification using the sparQ Universal Library Quant kit (QuantaBio) for Illumina sequencing.
146 The libraries were diluted to 10 pM and sequenced on an Illumina MiSeq instrument (V3
147 chemistry, PE300) with 1% PhiX as internal control.

148

149 **Bioinformatic analysis**

150 The Illumina sequencing output files were demultiplexed using bcl2fastq (v2.20.0.422) to
151 convert into FASTQ files. Initial quality control was performed through FastQ Screen.²⁴ Samples
152 were then processed using the UB Genomics and Bioinformatics Core SARS-CoV-2 analysis
153 pipeline (<https://github.com/UBGBC/fastq-to-consensus>). Briefly, adapters were trimmed before
154 sequencing reads were aligned to the SARS-CoV-2 reference genome (MN908947.2) using the
155 BWA-MEM algorithm.²⁵ Variants, insertions, and deletions were then called using BCFtools
156 (v.1.10.2),²⁶ requiring a minimum depth per nucleotide position of 10× or 50× and generating VCF
157 file outputs along with a final consensus FASTA file for each input sample. The resulting VCF
158 and depth mpileup files were used as input into Freyja to perform lineage composition analysis
159 (<https://github.com/andersen-lab/Freyja>).⁵ The coverage (--covcut) was specified at 10× or 50×,
160 and only confirmed lineages were reported. The Freyja pipeline was selected because of its high
161 accuracy and efficiency.⁵

162

163 **Patient-derived SARS-CoV-2 data**

164 The daily cases of COVID-19 during the sampling periods in the studied sewersheds were
165 extracted from the Erie County Wastewater Monitoring Dashboard.²⁷ The COVID-19 incidence
166 rates (per 100 000 population in the sewershed) were then calculated as 7-day rolling averages.

167 The patient-derived WGS data at the County level were downloaded from the Global Initiative on
168 Sharing All Influenza Data (GISAID) database²⁸ with the location as “North America/USA/New
169 York/Erie County,” collection date from “2021-10-01” to “2022-04-30”, and low coverage
170 excluded (GISAID Identifier: EPI_SET_220906wr). Most of these samples were sequenced at
171 University at Buffalo.²⁹ On each collection date, the relative abundances of SARS-CoV-2 lineages
172 in the patient samples were calculated, and the number of patient samples that were collected for
173 sequencing were smoothed as 7-day rolling averages.

174

175 **Statistical analysis**

176 The probability of recovering >90% coverage of the SARS-CoV-2 genome at 10× depth at
177 a given RT-qPCR C_T value or COVID-19 incidence rate was predicted by binary logistic
178 regression analysis. Data were visualized with Prism 9.2.0 (GraphPad Software) and the ggplot2³⁰
179 package in R version 4.2.1.³¹

180

181 **Data availability**

182 Raw sequencing data are available in NCBI Sequence Read Archive (SRA) under the
183 BioProject ID: PRJNA877272. Codes for analyzing SARS-CoV-2 lineage in wastewater are
184 available at <https://github.com/UBGBC/fastq-to-consensus>.

185

186 **RESULTS AND DISCUSSION**

187 **Coverage and depth of SARS-CoV-2 genomes from wastewater**

188 Complete or near-complete SARS-CoV-2 genomes (>90% coverage) at 10× depth were
189 recovered from 68% (64/94) of the wastewater samples (**Table S4**). This success rate is 53% higher

190 than that in a SARS-CoV-2 wastewater sequencing study that applied aluminum hydroxide
191 flocculation and the ARTIC protocol.¹⁴ A binary logistic regression analysis predicted a 0.9
192 probability of sequencing success (>90% coverage at 10× depth) when the C_T value of the SARS-
193 CoV-2 N gene was 31.8 (corresponding to ~3500 gene copies loaded for sequencing) (**Figure 1A**).
194 For comparison, at the 0.9 probability of sequencing success, C_T values of SARS-CoV-2 gene
195 ranged from <26 to ~29 with other workflows in previous pilot studies (**Figure S6**).¹⁴⁻¹⁷ Our
196 workflow demonstrates higher coverage of SARS-CoV-2 genome at higher C_T values (lower gene
197 levels).

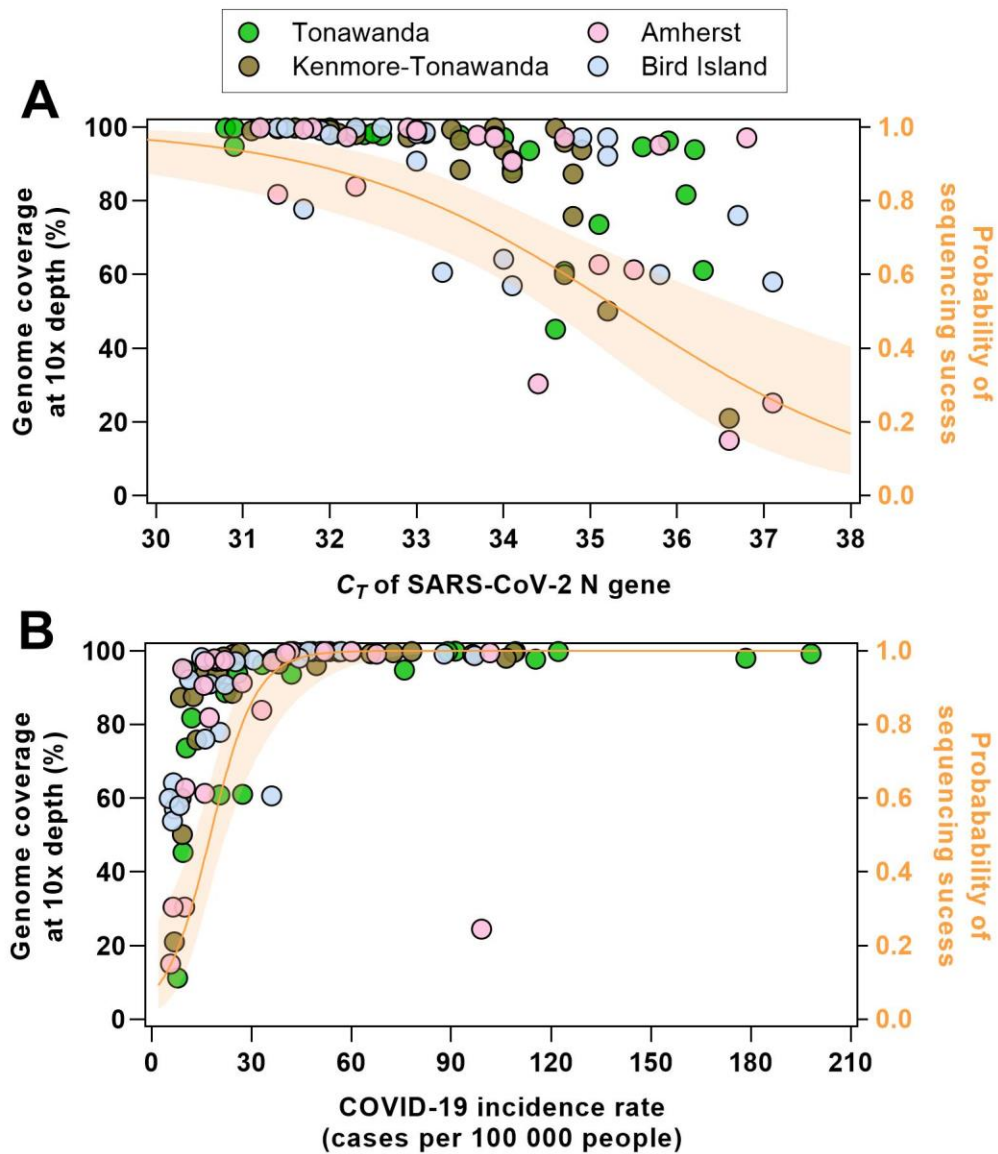
198 Most genomic regions were sequenced at a minimum depth of 50× (**Figure S7**). We noted
199 that three regions were often sequenced at lower depth (<10×): nucleotides 21750 to 22250 in the
200 S gene (amplicons 72 and 73) and 26750 to 27000 in the M gene (amplicon 89) (**Figure S7**).
201 Similar amplicon dropout issues were previously reported for a few amplicons using the ARTIC
202 V3 panel.^{32, 33} We used ARTIC V4.0 primers, which address the V3 coverage issues but do not
203 include all the mutations in SARS-CoV-2 Delta and Omicron lineages in the primer design.³⁴ Other
204 wastewater factors may also explain the low-depth coverage within certain regions of SARS-CoV-
205 2 genome. First, the low concentrations of the SARS-CoV-2 genome in wastewater (<10⁵ gene
206 copies/mL)³⁵ may have contributed to the lower sequencing depth. The presence of primer dimers
207 compete for primer-template interactions, resulting in reduced amplification efficiency.³⁶ Also,
208 mutations of SARS-CoV-2 genomes identified in wastewater but not in patient samples could
209 influence primer binding at some sites.^{3, 6, 37} Our results suggest that up-to-date primer design and
210 optimization is critical to sequence emerging variants from wastewater.

211

212 **Robustness of SARS-CoV-2 WGS from wastewater**

213 *Influence of sewersheds.* The rates of sequencing success were similar for samples
214 collected from the four studied sewersheds: 70.8% (17/24) for Tonawanda, 72.0% (18/25) for
215 Kenmore-Tonawanda, 72.7% (16/22) for Amherst, and 65.2% (15/23) for Bird Island (**Table S4**).
216 Although the Bird Island sewershed serves a population that is larger than the other three (**Table**
217 **S1**), similar average C_T values were obtained for the SARS-CoV-2 N gene (33.5 for Tonawanda,
218 33.4 for Kenmore-Tonawanda, 34.2 for Amherst, and 34.1 for Bird Island) (**Table S4**), indicating
219 that similar genome levels were available for sequencing. Notably, the Bird Island wastewater
220 treatment plant collects wastewater exclusively through combined sewer systems (**Table S1**). A
221 large fraction of sequencing inhibitors, such as humic acids and heavy metals, in the stormwater
222 runoff may slightly reduce the WGS success rate.^{38, 39}

223 *Influence of COVID-19 incidence.* The probability of sequencing success was >0.9 when
224 the COVID-19 incidence rate was >33/100 000 persons but decreased to 0.75 when the incidence
225 rate was 25.2/100 000 persons (**Figure 1B**). A previous study reported a probability of 0.75 to
226 quantify SARS-CoV-2 gene in wastewater by RT-qPCR when the 14-day COVID-19 case rate
227 was 152/100 000 persons.⁴⁰ In that study, viruses were concentrated from solids-removed influent
228 samples by 10-kDa Centricon ultra-filters.⁴⁰ We are not aware of other wastewater sequencing
229 studies that have calculated SARS-CoV-2 WGS success rates with regard to the incidence rate,
230 but our results suggest that SARS-CoV-2 WGS with the viruses recovered by tangential-flow
231 filtration method can be successfully applied at low COVID-19 incidence rates.



232

233 **Figure 1.** Coverage of the SARS-CoV-2 genome at 10× depth and the probability of sequencing
 234 success (>90% coverage at 10× depth) with regard to C_T value of the SARS-CoV-2 N gene
 235 measured with RT-qPCR (A) and the COVID-19 incidence rate (rolling 7-day average of cases
 236 per 100 000 people) (B). The probability of sequencing success was calculated according to a
 237 binary logistic regression analysis.

238

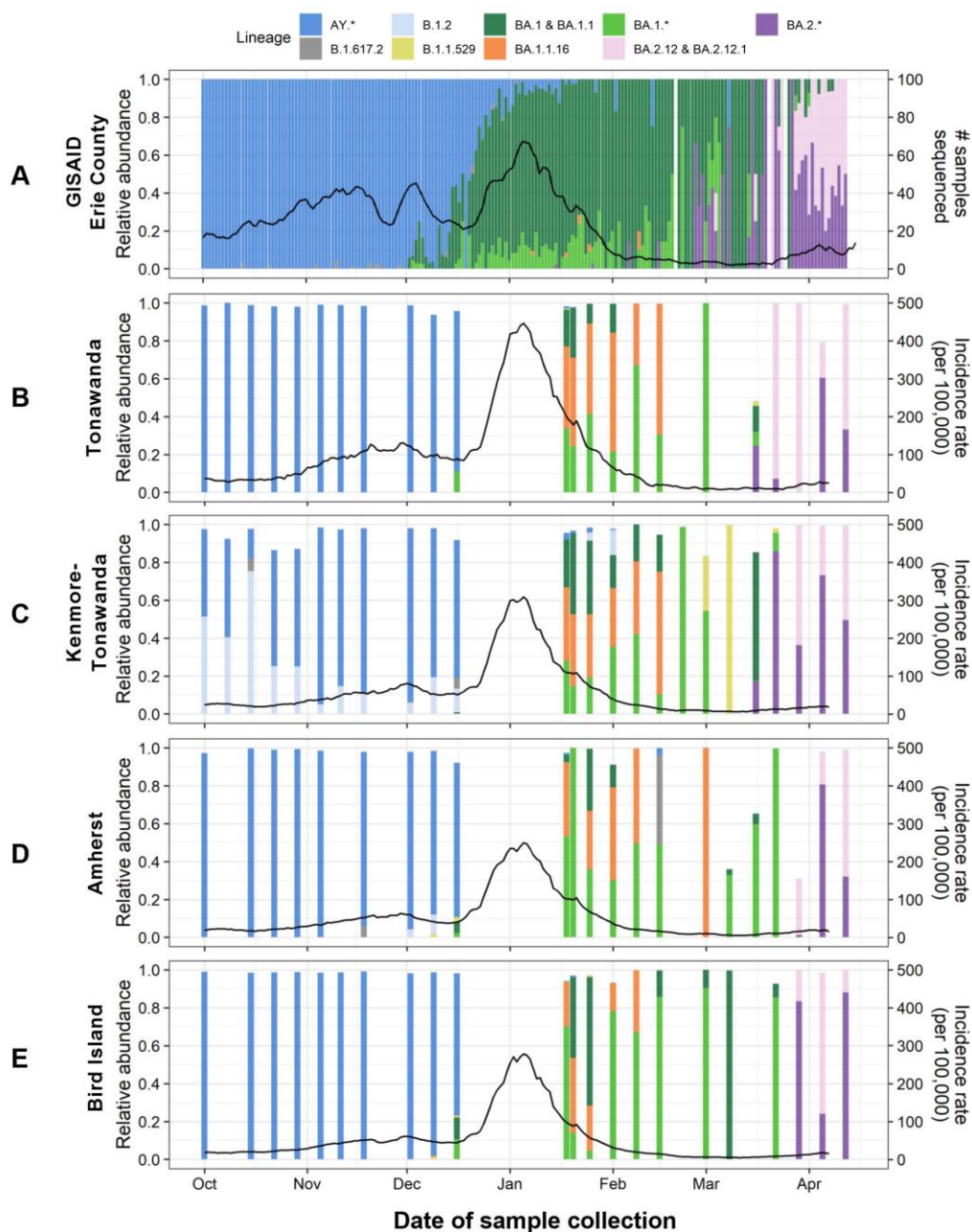
239 **Lineage distributions estimated by wastewater and clinical data**

240 Most of our wastewater samples were sequenced to an average depth of >50× per 250-
241 nucleotide-region across the genome (**Figure S7**). Although the estimated lineage abundances at
242 sequencing depths of 10× and 50× were very similar (**Figure S8**), we only reported lineage
243 distributions estimated by the WGS data filtered at a depth of 50×.

244 Nine dominant groups of lineages were identified in the wastewater samples: AY.* (Delta),
245 B.1.617.2 (Delta), B.1.2, B.1.1.529 (Omicron), BA.1/BA.1.1 (Omicron), BA.1.1.16 (Omicron),
246 other BA.1.* (Omicron), BA.2.12/BA.2.12.1 (Omicron), and other BA.2.* (Omicron). The
247 prevalence of Delta AY.* lineages in wastewater in October–December 2021 was coincident with
248 the lineages observed via clinical surveillance (**Figure 2**). Two Omicron infection waves in 2022
249 (BA.1 in January/February and BA.2 in March/April) predicted from the wastewater data aligned
250 with clinical data (**Figure 2**). Remarkably, wastewater sequencing revealed lineages that were
251 underrepresented or not present in the clinical data. Specifically, the B.1.2 lineage was abundant
252 in the Kenmore-Tonawanda sewershed in October but was not detected in patient samples from
253 that time (**Figure 2A**). Moreover, in January/February of 2022, the BA.1/BA.1.1 lineages were
254 prevalent in patient samples (**Figure 2A**), whereas the BA.1.1.16 lineage dominated in the
255 wastewater samples (**Figure 2B–E**). Notably, the genome sequences of the BA.1/BA.1.1 and
256 BA.1.1.16 lineages are similar, which might affect the predictions of their relative abundance.

257 The reason that B.1.2 lineage identified in wastewater samples but largely absent from
258 patient samples is unclear. The Freyja pipeline identified B.1.2 on the basis of a mutation
259 spectrum, consisting of 13 nucleotide substitutions (A18424G, A23403G, C10319T, C1059T,
260 C14408T, C21304T, C241T, C27964T, C28472T, C28869T, C3037T, G25563T, and G25907T),

261 three of which (C1059T, C21304T, and G25563T) overlap the mutations in highly abundant
262 Delta lineages circulating at the time. Furthermore, the B.1.2 mutation spectrum does not share a
263 strong correlation with any of the mutation spectra of Delta lineages (**Figure S9**). This is less
264 likely a misassignment by the pipeline. Taken together, our findings suggest that the WGS of
265 patient samples can miss SARS-CoV-2 lineages circulating in the community. Those lineages
266 may not be clinically relevant, but future research is needed to understand their roles in viral
267 evolution and lineage emergence.



268

269 **Figure 2.** Distributions of dominant SARS-CoV-2 lineages estimated from Erie County clinical
 270 data deposited on GISAID (A) and wastewater sequencing data (B–E) during the sampling periods.

271 The solid black lines represent the rolling 7-day average numbers of clinical samples collected for
 272 sequencing (A) and COVID-19 incidence rates (cases per 100 000 people) in each sewershed (B–

273 E).

274

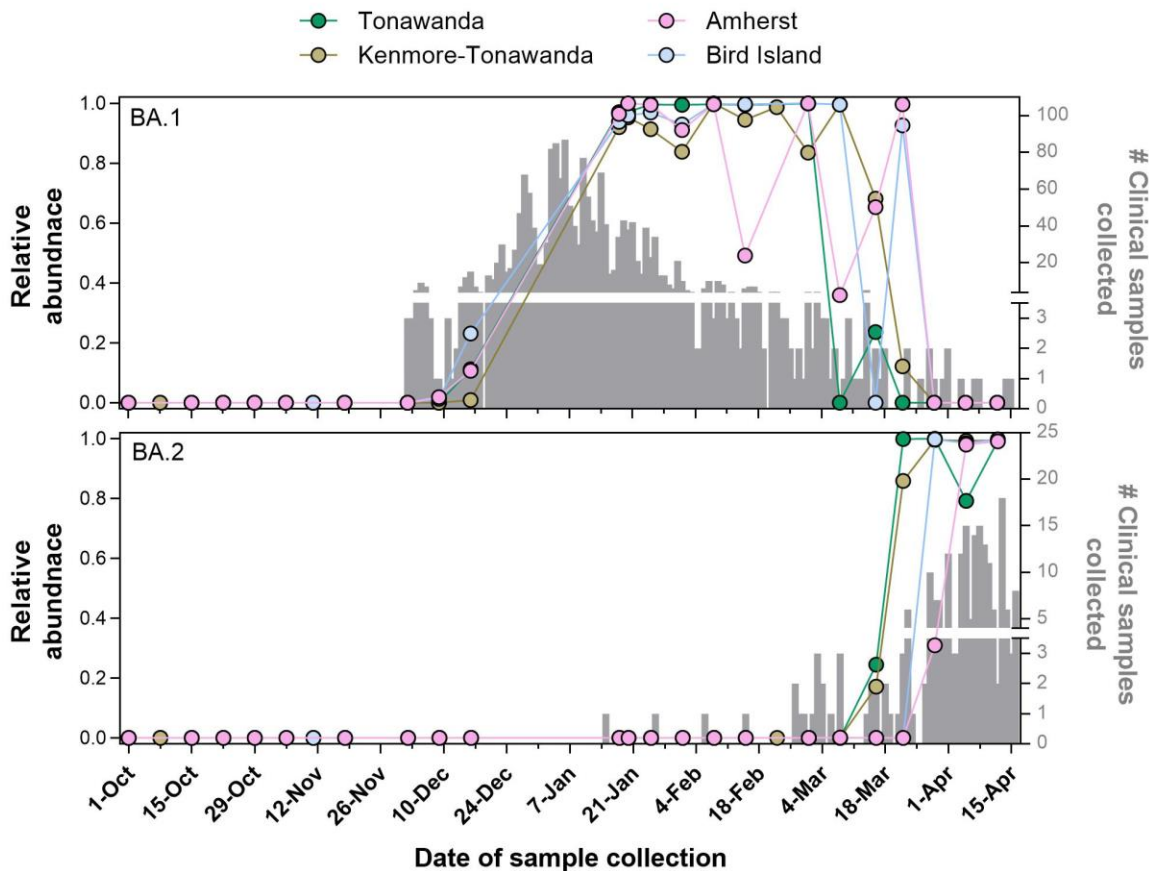
275 **Early detection of variants in wastewater**

276 The values of early detection of SARS-CoV-2 variants in wastewater depend on the delays
277 in clinical analysis.⁴¹ The workflow optimization for a quick turnaround of WGS analysis is
278 beyond the scope of this study. Here, we only compare the detection of emerging SARS-CoV-2
279 variants based on the date of collection for both wastewater and patient samples.

280 The Omicron BA.1 was first identified in Amherst and Bird Island wastewater with a
281 relative abundance of 1-2% in the second week of December, which is ~1 week later than the
282 patient-derived samples (**Figure 3**). The detection of Omicron BA.2 from wastewater samples in
283 March was similarly delayed (**Figure 3**). Note that some BA.2 patient-derived samples were
284 collected in January and February, but there was no Omicron BA.2 outbreak until March. The poor
285 detection of Omicron BA.2 in wastewater may be attributable to the relatively low coverage of the
286 SARS-CoV-2 genome from wastewater during mid-February and early March (<65%; Table S3).
287 Nevertheless, our findings suggest that wastewater is a relevant proxy for patient samples.
288 Wastewater WGS should be considered in the face of practical delays in clinical sequencing for
289 early detection of variants.

290 We found that RT-qPCR assays were more sensitive than wastewater WGS for detecting
291 Omicron BA.1-specific mutations, but wastewater WGS was more sensitive for Omicron BA.2-
292 specific mutations (**Table S4**). However, RT-qPCR assays are less sensitive than digital PCR
293 assays,⁴² which were reported to detect variant-specific mutations earlier than genetic sequencing.⁹
294 Interestingly, our RT-qPCR assays detected S:delH69/V70 mutations (for Omicron BA.1) in the
295 Kenmore-Tonawanda wastewater samples collected in October 2021. Although WGS also
296 detected these mutations, other Omicron-specific mutations in the S gene (Q493R and Q498R)

297 were not detected at the time. Wastewater WGS may thus be more precise than PCR assays for
 298 early detection of SARS-CoV-2 variants.



299
 300 **Figure 3.** Detection of Omicron BA.1 and BA.2 in wastewater and clinical samples. The relative
 301 abundance of Omicron was predicted by Freyja pipeline with the wastewater sequencing data
 302 filtered at 50× depth. The relative abundance of BA.1 (top) is the sum of relative abundances of
 303 B.1.1.529, BA.1, BA.1.1, and other BA.1.*. The relative abundance of BA.2 (bottom) comprises
 304 BA.2.12, BA.2.12.1, and other BA.2.*. The number of clinical samples collected for sequencing
 305 was counted on every collection date.

306

307 **CONCLUSIONS**

308 Our research demonstrates that tangential-flow filtration to concentrate viruses from
309 wastewater samples enables extraction of nucleic acids of high-enough quality for stable
310 performance of SARS-CoV-2 WGS. Complete or near-complete genomes at a depth of 10× were
311 sequenced from 68% (64/94) of the wastewater samples. Moreover, the tangential-flow filtration
312 method improves the WGS success at lower COVID-19 incidence rates. Our results report a 0.9
313 probability of WGS success when the COVID-19 incidence rate exceeded 33/100 000 persons.
314 Furthermore, WGS of SARS-CoV-2 in wastewater revealed lineages underrepresented or not
315 detected from patient samples. Future studies are needed to advance wastewater WGS data
316 interpretation and streamline the workflow of wastewater WGS to shorten the turnaround time for
317 early detection.

318 The developed reusable and likely cost-effective tangential-flow filtration method is
319 readily applicable to other sequencing assays that requires high-quality viral nucleic acids from
320 wastewater. Given the flexibility of concentrating large volumes of wastewater, the tangential-
321 flow filtration system can be further optimized for genomic surveillance of low-abundance viruses
322 in wastewater.

323

324 **ASSOCIATED CONTENT**

325 **Supporting information**

326 The supporting information is available free of charge at <http://pubs.acs.org>.

327 Inhibition test; RT-qPCR assay details and Limit of detection (LOD) and limit of
328 quantification (LOQ) determination; Details of four sewersheds in this study; Table S2.
329 Details of RT-qPCR assay for quantifying SARS-CoV-2 N gene and S gene mutations;

330 Check list of RT-qPCR experiments according to the MIQE (minimum information for
331 publication of quantitative real-time PCR experiments) guidelines; Summary of
332 wastewater samples sequenced in this study; Geographic locations of four sewersheds in
333 Erie County, New York; Schematic of tangential-flow filtration system; SARS-CoV-2 N
334 gene levels in wastewater and blank test samples; Determination of limit of detection
335 (LOD; left) and limit of quantification (LOQ; right) of SARS-CoV-2 N gene by RT-qPCR;
336 RT-qPCR inhibition test of SARS-CoV-2 N gene in the wastewater nucleic acid extracts;
337 Comparison of SARS-CoV-2 genome coverage from wastewater with different workflows;
338 Heat map of read depths of SARS-CoV-2 whole-genome sequencing from wastewater
339 samples; Comparison of relative abundances of SARS-CoV-2 lineages estimated by the
340 sequencing data at depths of 10× and 50×; Pair-wise pearson correlation of B.1.2 lineage
341 mutaton spectrum against all other lineage mutation spectra.

342

343 **ACKNOWLEDGEMENTS**

344 This work was funded by Erie County Department of Health (ECDOH) award 91287 to Y.Y. and
345 I.M.B. and award 91279 to J.A.S.. We thank undergraduate students Vicky Huang and Danya
346 Hanin for processing the wastewater samples in the lab. We also thank Joseph L. Fiegl for
347 coordinating the wastewater sample collection. The GISAID data used in the manuscript
348 (Identifier: EPI_SET_220906wr) is composed of 4952 individual genome sequences published in
349 GISAID’s EpiCoV database. To view the contributors of each individual sequence with details,
350 visit doi.org/10.55876/gis8.220906wr. Most of the samples (4653/4952) were sequenced at the
351 University at Buffalo. We are grateful for the sequencing work of scientists and healthcare
352 professionals who generated the remaining sequences from the region and made them publicly
353 accessible through GISAID.

354 **REFERENCES**

355

- 356 (1) Walensky, R. P.; Walke, H. T.; Fauci, A. S. SARS-CoV-2 variants of concern in the United States-
357 challenges and opportunities. *JAMA* **2021**, *325* (11), 1037-1038. DOI: 10.1001/jama.2021.2294.
- 358 (2) Oude Munnink, B. B.; Nieuwenhuijse, D. F.; Stein, M.; O'Toole, A.; Haverkate, M.; Mollers, M.; Kamga,
359 S. K.; Schapendonk, C.; Pronk, M.; Lexmond, P.; et al. Rapid SARS-CoV-2 whole-genome sequencing and
360 analysis for informed public health decision-making in the Netherlands. *Nat Med* **2020**, *26* (9), 1405-
361 1410. DOI: 10.1038/s41591-020-0997-y.
- 362 (3) Crits-Christoph, A.; Kantor, R. S.; Olm, M. R.; Whitney, O. N.; Al-Shayeb, B.; Lou, Y. C.; Flamholz, A.;
363 Kennedy, L. C.; Greenwald, H.; Hinkle, A.; et al. Genome Sequencing of Sewage Detects Regionally
364 Prevalent SARS-CoV-2 Variants. *mBio* **2021**, *12* (1), e02703-e02720. DOI: 10.1128/mBio.02703-20.
- 365 (4) Nemudryi, A.; Nemudraia, A.; Wiegand, T.; Surya, K.; Buyukyoruk, M.; Cicha, C.; Vanderwood, K. K.;
366 Wilkinson, R.; Wiedenheft, B. Temporal Detection and Phylogenetic Assessment of SARS-CoV-2 in
367 Municipal Wastewater. *Cell Rep Med* **2020**, *1* (6), 100098. DOI: 10.1016/j.xcrm.2020.100098.
- 368 (5) Karthikeyan, S.; Levy, J. I.; De Hoff, P.; Humphrey, G.; Birmingham, A.; Jepsen, K.; Farmer, S.; Tubb, H.
369 M.; Valles, T.; Tribelhorn, C. E.; et al. Wastewater sequencing reveals early cryptic SARS-CoV-2 variant
370 transmission. *Nature* **2022**, *609*, 101-108. DOI: 10.1038/s41586-022-05049-6.
- 371 (6) Smyth, D. S.; Trujillo, M.; Gregory, D. A.; Cheung, K.; Gao, A.; Graham, M.; Guan, Y.; Guldenpfennig,
372 C.; Hoxie, I.; Kannoly, S.; et al. Tracking cryptic SARS-CoV-2 lineages detected in NYC wastewater. *Nature*
373 *Commun* **2022**, *13* (1), 1-9. DOI: 10.1038/s41467-022-28246-3.
- 374 (7) Sims, D.; Sudbery, I.; Illott, N. E.; Heger, A.; Ponting, C. P. Sequencing depth and coverage: key
375 considerations in genomic analyses. *Nat Rev Genet* **2014**, *15* (2), 121-132. DOI: 10.1038/nrg3642.
- 376 (8) Valieris, R.; Drummond, R. D.; Defelicibus, A.; Dias-Neto, E.; Rosales, R. A.; Tojal da Silva, I. A mixture
377 model for determining SARS-Cov-2 variant composition in pooled samples. *Bioinformatics* **2022**, *38* (7),
378 1809-1815. DOI: 10.1093/bioinformatics/btac047.
- 379 (9) Lou, E. G.; Sapoval, N.; McCall, C.; Bauhs, L.; Carlson-Stadler, R.; Kalvapalle, P.; Lai, Y.; Palmer, K.;
380 Penn, R.; Rich, W.; et al. Direct comparison of RT-ddPCR and targeted amplicon sequencing for SARS-
381 CoV-2 mutation monitoring in wastewater. *Sci Total Environ* **2022**, 155059. DOI:
382 10.1016/j.scitotenv.2022.155059.
- 383 (10) Graham, K. E.; Loeb, S. K.; Wolfe, M. K.; Catoe, D.; Sinnott-Armstrong, N.; Kim, S.; Yamahara, K. M.;
384 Sassoubre, L. M.; Grijalva, L. M. M.; Roldan-Hernandez, L.; et al. SARS-CoV-2 RNA in wastewater settled
385 solids is associated with COVID-19 cases in a large urban sewershed. *Environ Sci Technol* **2021**, *55* (1),
386 488-498. DOI: 10.1021/acs.est.0c06191.
- 387 (11) LaTurner, Z. W.; Zong, D. M.; Kalvapalle, P.; Gamas, K. R.; Terwilliger, A.; Crosby, T.; Ali, P.;
388 Avadhanula, V.; Santos, H. H.; Weesner, K.; et al. Evaluating recovery, cost, and throughput of different
389 concentration methods for SARS-CoV-2 wastewater-based epidemiology. *Water Res* **2021**, *197*, 117043.
390 DOI: 10.1016/j.watres.2021.117043.
- 391 (12) Zheng, X.; Deng, Y.; Xu, X.; Li, S.; Zhang, Y.; Ding, J.; On, H. Y.; Lai, J. C. C.; In Yau, C.; Chin, A. W. H.; et
392 al. Comparison of virus concentration methods and RNA extraction methods for SARS-CoV-2 wastewater
393 surveillance. *Sci Total Environ* **2022**, *824*, 153687. DOI: 10.1016/j.scitotenv.2022.153687.
- 394 (13) Peccia, J.; Zulli, A.; Brackney, D. E.; Grubaugh, N. D.; Kaplan, E. H.; Casanovas-Massana, A.; Ko, A. I.;
395 Malik, A. A.; Wang, D.; Wang, M.; et al. Measurement of SARS-CoV-2 RNA in wastewater tracks
396 community infection dynamics. *Nat Biotechnol* **2020**, *38* (10), 1164-1167. DOI: 10.1038/s41587-020-
397 0684-z.
- 398 (14) Perez-Cataluna, A.; Chiner-Oms, A.; Cuevas-Ferrando, E.; Diaz-Reolid, A.; Falco, I.; Randazzo, W.;
399 Giron-Guzman, I.; Allende, A.; Bracho, M. A.; Comas, I.; et al. Spatial and temporal distribution of SARS-

400 CoV-2 diversity circulating in wastewater. *Water Res* **2022**, *211*, 118007. DOI:
401 10.1016/j.watres.2021.118007.

402 (15) Fontenele, R. S.; Kraberger, S.; Hadfield, J.; Driver, E. M.; Bowes, D.; Holland, L. A.; Faleye, T. O. C.;
403 Adhikari, S.; Kumar, R.; Inchausti, R.; et al. High-throughput sequencing of SARS-CoV-2 in wastewater
404 provides insights into circulating variants. *Water Res* **2021**, *205*, 117710. DOI:
405 10.1016/j.watres.2021.117710.

406 (16) Bar-Or, I.; Weil, M.; Indenbaum, V.; Bucris, E.; Bar-Ilan, D.; Elul, M.; Levi, N.; Aguvaev, I.; Cohen, Z.;
407 Shirazi, R.; et al. Detection of SARS-CoV-2 variants by genomic analysis of wastewater samples in Israel.
408 *Sci Total Environ* **2021**, *789*, 148002. DOI: 10.1016/j.scitotenv.2021.148002.

409 (17) Izquierdo-Lara, R.; Elsinga, G.; Heijnen, L.; Munnink, B. B. O.; Schapendonk, C. M. E.; Nieuwenhuijse,
410 D.; Kon, M.; Lu, L.; Aarestrup, F. M.; Lycett, S.; et al. Monitoring SARS-CoV-2 circulation and diversity
411 through community wastewater sequencing, the Netherlands and Belgium. *Emerg Infect Dis* **2021**, *27*
412 (5), 1405-1415. DOI: 10.3201/eid2705.204410.

413 (18) Lu, X.; Wang, L.; Sakthivel, S. K.; Whitaker, B.; Murray, J.; Kamili, S.; Lynch, B.; Malapati, L.; Burke, S.
414 A.; Harcourt, J.; et al. US CDC real-time reverse transcription PCR panel for detection of Severe Acute
415 Respiratory Syndrome Coronavirus 2. *Emerg Infect Dis* **2020**, *26* (8), 1654. DOI:
416 10.3201/eid2608.201246.

417 (19) Lee, W. L.; Gu, X.; Armas, F.; Wu, F.; Chandra, F.; Chen, H.; Xiao, A.; Leifels, M.; Chua, F. J. D.; Kwok,
418 G. W. C.; et al. Quantitative detection of SARS-CoV-2 Omicron BA.1 and BA.2 variants in wastewater
419 through allele-specific RT-qPCR. *medRxiv* **2022**. DOI: 10.1101/2021.12.21.21268077.

420 (20) Lee, W. L.; Imakaev, M.; Armas, F.; McElroy, K. A.; Gu, X. Q.; Duvallet, C.; Chandra, F.; Chen, H. J.;
421 Leifels, M.; Mendola, S.; et al. Quantitative SARS-CoV-2 Alpha variant B.1.1.7 tracking in wastewater by
422 allele-specific RT-qPCR. *Environ Sci Technol Lett* **2021**, *8* (8), 675-682. DOI: 10.1021/acs.estlett.1c00375.

423 (21) He, H.; Zhou, P.; Shimabuku, K. K.; Fang, X.; Li, S.; Lee, Y.; Dodd, M. C. Degradation and deactivation
424 of bacterial antibiotic resistance genes during exposure to free chlorine, monochloramine, chlorine
425 dioxide, ozone, ultraviolet light, and hydroxyl radical. *Environ Sci Technol* **2019**, *53* (4), 2013-2026. DOI:
426 10.1021/acs.est.8b04393.

427 (22) Bustin, S. A.; Benes, V.; Garson, J. A.; Hellemans, J.; Huggett, J.; Kubista, M.; Mueller, R.; Nolan, T.;
428 Pfaffl, M. W.; Shipley, G. L.; et al. The MIQE guidelines: minimum information for publication of
429 quantitative real-time PCR experiments. *Clin Chem* **2009**, *55* (4), 611-622. DOI:
430 10.1373/clinchem.2008.112797.

431 (23) *nCoV-2019 sequencing protocol V.1*. 2020. [https://www.protocols.io/view/ncov-2019-sequencing-
432 protocol-bp2l6n26rgqe/v1?version_warning=no](https://www.protocols.io/view/ncov-2019-sequencing-protocol-bp2l6n26rgqe/v1?version_warning=no) (accessed 2020-01-22).

433 (24) Wingett, S. W.; Andrews, S. FastQ Screen: A tool for multi-genome mapping and quality control.
434 *F1000Research* **2018**, *7*, 1338. DOI: 10.12688/f1000research.15931.2.

435 (25) Li, H.; Durbin, R. Fast and accurate short read alignment with Burrows-Wheeler transform.
436 *Bioinformatics* **2009**, *25* (14), 1754-1760. DOI: 10.1093/bioinformatics/btp324.

437 (26) Danecek, P.; Bonfield, J. K.; Liddle, J.; Marshall, J.; Ohan, V.; Pollard, M. O.; Whitwham, A.; Keane, T.;
438 McCarthy, S. A.; Davies, R. M.; et al. Twelve years of SAMtools and BCFtools. *Gigascience* **2021**, *10* (2).
439 DOI: 10.1093/gigascience/giab008 From NLM Medline.

440 (27) *Erie County SARS-CoV-2 wastewater monitoring dashboard*.
441 <https://erieny.maps.arcgis.com/apps/dashboards/a95853269eec489ea59e5b71571f2e76> (accessed
442 2022-04-15).

443 (28) Elbe, S.; Buckland-Merrett, G. Data, disease and diplomacy: GISAID's innovative contribution to
444 global health. *Glob Chall* **2017**, *1* (1), 33-46. DOI: 10.1002/gch2.1018.

445 (29) Lamb, N. A.; Bard, J.E.; Pohlman, A.; Boccolucci, A.; Yergeau, D.A.; Marzullo, B.J.; Pope, C.; Burstein,
446 G.; Tomaszewski, J.; Nowak, N.J. and Surtees, J.A. Genomic Surveillance of SARS-CoV-2 in Erie County,
447 New York. *medRxiv* **2021**. DOI: 10.1101/2021.07.01.21259869.

- 448 (30) Wickham, H. *ggplot2: Elegant Graphics for Data Analysis*; Springer-Verlag New York, 2016.
- 449 (31) Team, R. C. *RStudio: Integrated Development for R*. RStudio; PBC, Boston, MA, 2020.
- 450 (32) Jahn, K.; Dreifuss, D.; Topolsky, I.; Kull, A.; Ganesanandamoorthy, P.; Fernandez-Cassi, X.; Bänziger,
451 C.; Devaux, A. J.; Stachler, E.; Caduff, L.; et al. Early detection and surveillance of SARS-CoV-2 genomic
452 variants in wastewater using COJAC. *Nat Microbiol* **2022**, 1-10. DOI: 10.1038/s41564-022-01185-x.
- 453 (33) Lambisia, A. W.; Mohammed, K. S.; Makori, T. O.; Ndwiga, L.; Mburu, M. W.; Morobe, J. M.; Moraa,
454 E. O.; Musyoki, J.; Murunga, N.; Mwangi, J. N.; et al. Optimization of the SARS-CoV-2 ARTIC Network V4
455 Primers and Whole Genome Sequencing Protocol. *Front Med (Lausanne)* **2022**, 9, 836728. DOI:
456 10.3389/fmed.2022.836728.
- 457 (34) Clark, C. R.; Hardison, M. T.; Houdeshell, H. N.; Vest, A. C.; Whitlock, D. A.; Skola, D. D.; Koble, J. S.;
458 Oberholzer, M.; Schroth, G. P. Evaluation of an optimized protocol and Illumina ARTIC V4 primer pool for
459 sequencing of SARS-CoV-2 using COVIDSeq™ and DRAGEN™ COVID Lineage App workflow. *bioRxiv* **2022**.
460 DOI: 10.1101/2022.01.07.475443.
- 461 (35) Mantilla-Calderon, D.; Huang, K. Y.; Li, A. J.; Chibwe, K.; Yu, X. Q.; Ye, Y.; Liu, L.; Ling, F. Q. Emerging
462 investigator series: meta-analyses on SARS-CoV-2 viral RNA levels in wastewater and their correlations
463 to epidemiological indicators. *Environ Sci: Wat Res Technol* **2022**, 8 (7), 1391-1407. DOI:
464 10.1039/d2ew00084a.
- 465 (36) Itokawa, K.; Sekizuka, T.; Hashino, M.; Tanaka, R.; Kuroda, M. Disentangling primer interactions
466 improves SARS-CoV-2 genome sequencing by multiplex tiling PCR. *PLoS One* **2020**, 15 (9), e0239403.
467 DOI: 10.1371/journal.pone.0239403.
- 468 (37) Agrawal, S.; Orschler, L.; Lackner, S. Metatranscriptomic analysis reveals SARS-CoV-2 mutations in
469 wastewater of the Frankfurt metropolitan area in southern Germany. *Microbiol Resour Announc* **2021**,
470 10 (15), e00280-00221. DOI: 10.1128/MRA.00280-21.
- 471 (38) Grant, S. B.; Rekhi, N. V.; Pise, N. R.; Reeves, R. L.; Matsumoto, M.; Wistrom, A.; Moussa, L.; Bay, S.;
472 Kayhanian, M. A review of the contaminants and toxicity associated with particles in stormwater runoff.
473 *Terminology* **2003**, 2 (2), 1-173.
- 474 (39) Schrader, C.; Schielke, A.; Ellerbroek, L.; Johne, R. PCR inhibitors - occurrence, properties and
475 removal. *J Appl Microbiol* **2012**, 113 (5), 1014-1026. DOI: 10.1111/j.1365-2672.2012.05384.x.
- 476 (40) Tiwari, A.; Lipponen, A.; Hokajarvi, A. M.; Luomala, O.; Sarekoski, A.; Ryttonen, A.; Osterlund, P.; Al-
477 Hello, H.; Juutinen, A.; Miettinen, I. T.; et al. Detection and quantification of SARS-CoV-2 RNA in
478 wastewater influent in relation to reported COVID-19 incidence in Finland. *Water Res* **2022**, 215,
479 118220. DOI: 10.1016/j.watres.2022.118220.
- 480 (41) Larsen, D. A.; Wigginton, K. R. Tracking COVID-19 with wastewater. *Nat Biotechnol* **2020**, 38 (10),
481 1151-1153. DOI: 10.1038/s41587-020-0690-1.
- 482 (42) Ahmed, W., Smith, W.J., Metcalfe, S., Jackson, G., Choi, P.M., Morrison, M., Field, D., Gyawali, P.,
483 Bivins, A., Bibby, K. and Simpson, S.L. Comparison of RT-qPCR and RT-dPCR platforms for the trace
484 detection of SARS-CoV-2 RNA in wastewater. *ACS ES&T Water* **2022**. DOI: 10.1021/acsestwater.1c00387.

485